ACS APPLIED MATERIALS & INTERFACES

Research Article

www.acsami.org

Dynamic Moisture Sorption Characteristics of Xerogels from Water-Swellable Oligo(oxyethylene) Lignin Derivatives

Lars Passauer,*[,†,‡] Marlene Struch,[†,§] Stefan Schuldt,[⊥] Joern Appelt,[†,#] Yvonne Schneider,[⊥] Doris Jaros,[⊥] and Harald Rohm[⊥]

[†]Institute of Plant and Wood Chemistry, Technische Universitaet Dresden, Dresden, Germany

[‡]Dresden Institute of Wood Technology - Institut fuer Holztechnologie Dresden gemeinnuetzige GmbH, Dresden, Germany

[⊥]Institute of Food Technology and Bioprocessing Engineering, Technische Universitaet Dresden, Dresden, Germany

ABSTRACT: Highly swellable lignin derivatives were prepared by cross-linking of oxidatively preactivated spruce organosolv lignin (OSL) with poly(ethylene) glycol diglycidyl ether (PEGDGE). The lignin gels obtained are considered to be an environmentally friendly alternative to synthetic hydrogels and superabsorbents and represent a novel type of lignin based functional materials. For their application, it is not only the absorption of water in terms of hydrogel swelling that plays an important role, but also the adsorption and retention of moisture by the corresponding xerogels. To reveal the mechanisms involved in moistening and reswelling of the lignin gels, the interaction of water vapor with lyophilized xerogels was investigated and compared with sorption characteristics of parent lignin. The chemical structure of PEGDGE-modified lignin was investigated using attenuated total reflectance Fourier-transformed infrared spectroscopy and selective aminolysis and was related to its sorption and swelling characteristics. Bound and free water in hydrogels was determined by differential scanning calorimetry and by measuring the free swelling capacity of the gels. Moisture sorption of OSL and PEGDGE-modified lignin xerogels was determined using dynamic vapor sorption analysis. In order to determine monolayer and multilayer sorption parameters, sorption data were fitted to the Brunauer–Emmett–Teller and the Guggenheim–Anderson–de Boer model. Swelling properties of the hydrogels and moisture sorption of the corresponding xerogels were found to be strongly dependent on the degree of chemical modification with PEGDGE: Total and free water content of hydrogels decrease with increasing cross-linking density; on the other hand, water bound in hydrogels and moisture sorption of xerogels at high levels of water activity strongly increase, presumably because of the hydration of hydrophilic oligo(oxyethylene) and oligo(oxyethylene) glycol substituents, which lead to moisture diffusion into the xerogel matrix, plasticization, and swelling of the gels.

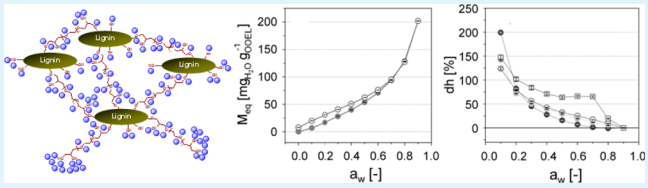

KEYWORDS: *organosolv lignin, poly(ethylene) glycol diglycidyl ether, phenolic hydroxyl groups, hydrogel, swelling capacity, xerogel, moisture sorption, BET, GAB*

1. INTRODUCTION

Next to cellulose, lignin is the second most abundant biopolymer on earth and a main constituent of the cell walls of supportive or conductive tissues of vascular plants that makes them rigid, impermeable, and resistant against decay.[1] It is biosynthesized by peroxidase induced random radical coupling of monolignols formed in the course of the shikimate pathway from glucose.[2] The phenolic building blocks, namely, *p*-coumaryl alcohol, coniferyl alcohol, and sinapyl alcohol, differ in the substitution of the 3 and 5 positions of the aromatic ring and are often referred to as C_9 or phenyl propane units.[2] Oxidative coupling of the aforementioned alcohols generates the predominant and labile β-O-4 bond, α-O-4 ether linkages, and more resistant C–C bonds (e.g., 5–5, β–5, and β–β linkages[3]), and as a consequence, a complex, heterogeneous, and hydrophobic cross-linked macromolecule.[1] Because of its structural complexity, the lack of stereoregularity and conjunctive binding to other substances, lignin is difficult to isolate and to convert into useful consumer products.[1,4] To date, technical lignin extracted from pulping liquors is mainly used as fuel in pulp production. Nevertheless, several attempts have been made to isolate and modify technical lignin to obtain highly valuable lignin-based products.[5−7] A special approach is the preparation of water-swellable lignin-based materials which may serve as environmental-friendly alternative to synthetic hydrogels and superabsorbents. The preparation of lignin hydrogels, however, requires a certain degree of chemical modification and/or cross-linking such as chemical cross-linking of kraft lignin, water-soluble lignosulfonates, or hydroxypropyl lignin[8] with formaldehyde,[9] glutaraldehyde,[10] α-epichlorhydrin,[11,] or diepoxy compounds.[8] Other approaches dealt with the copolymerization of acrylamide with lignin,[13] but all attempts resulting in gels with low water swelling capacities <10 g_{H2O} g^{-1}.[11−13] Besides Lindström's approach, the cross-

Received: July 31, 2012
Accepted: October 17, 2012
Published: October 17, 2012

   dx.doi.org/10.1021/am3015179 | *ACS Appl. Mater. Interfaces* 2012, 4, 5852–5862

linking of milled wood lignin[11] and kraft lignin[12] with epichlorhydrin, a promising work concerning lignin-based hydrogels, was communicated by Nishida et al.,[14,15] who reported chemical cross-linking of hardwood lignin with poly(ethylene) glycol diglycidyl ether (PEGDGE) and obtained hydrogels with a moderate swellability. Following that approach, Passauer et al.[16−20] achieved lignin hydrogels with a considerably increased free swelling capacity (FSC) up to 75 g_{H2O} g^{-1} by cross-linking of unmodified or oxidatively preactivated technical lignins with PEGDGE. Thus, the potential range of application of lignin gels has been broadened considerably. Among others, the intention is to utilize such lignin-based hydrogels as water storing soil amendment in agriculture and forestry for the rehabilitation of degraded soil,[20] where they enhance soil water binding but also contribute to soil fertility as natural ligneous source of humic substances.[16] For the potential application of these materials, it is not only the absorption of water in terms of swelling and reswelling of the hydrogels that plays an important role, but also the adsorption of water vapor by the corresponding xerogels which enables remoistening and reswelling of the xerogels after exposing them to dryness and, thus, the retention of water from the vapor phase.

Generally, the conversion of hydrogels into the xerogel form is linked to an unhindered dehydration and shrinkage of the cross-linked polymer. Xerogels usually show high porosity and specific surface along with pore sizes in the nanometer range.[21] Granular and porous materials retain water in both bound and free state as adsorbed monomolecular layer or as multilayers which, depending on moisture saturation, produce menisci with different configuration. With increasing moisture content, pendular, funicular, and capillary bridges between rigid particles are built.[22] The relationship between equilibrium moisture content M_{eq} of a material and the relative humidity RH of its surrounding is described by a moisture sorption isotherm,[23] which refers to moisture adsorption or desorption at a specific temperature. Depending on the material, hysteresis between adsorption and subsequent desorption reflects the extent to which chemical components of a material undergo structural and conformational rearrangements, which alter the number of energetically favorable sites, and result in water migration in the material during the sorption process.[24,25] In the context with moisture sorption phenomena, W.J. Scott introduced the concept of water activity in the early 1950s in which the relative water vapor pressure is related to the thermodynamic activity of water by $a_w = p/p_0$ = RH/100%, where a_w is the water activity derived from the laws of equilibrium of thermodynamics, p is the vapor pressure of the sample, and p_0 is the vapor pressure of pure water at the same temperature and external pressure.[26,27]

To explain moisture sorption in different matrices, numerous empirical, semiempirical or theoretical models were proposed, but none of these is universally expedient.[28,29] It is particularly the Brunauer−Emmett−Teller (BET) equation, which is widely used to simulate sorption processes in different physicochemical fields[23] because of its simplicity and because of its IUPAC approval.[29,30] An important modification of the BET equation is the Guggenheim−Anderson−de Boer (GAB) model, which has become popular in food technology.[29] Despite a recommendation by the European project group COST 90 on physical properties of foods and despite it covering almost the entire moisture sorption range ($0.05 \leq a_w \leq 0.8-0.9$), the GAB model is not well established in other applications.[29]

In a follow-up of our previous investigations, which mainly focused on rheological and swelling properties of PEGDGE-modified lignin hydrogels,[16,19,20] the aim of the current work is the chemical and physical characterization of the corresponding xerogels with the core area of moisture sorption characteristics and their relation to the microstructure and chemical structure of the gels. Total, free, and bound water fractions of swollen hydrogel counterparts were determined by free swelling capacity (FSC) measurement and differential scanning calorimetry (DSC). The chemical structure of parent and PEGDGE-modified lignin was investigated using selective aminolysis (in connection with gas chromatography GC) and attenuated total reflectance Fourier-transformed infrared spectroscopy (ATR FTIR). The microstructure of the materials was analyzed by scanning electron microscopy (SEM). To gain insight into the xerogel's sorption characteristics which play an important role in terms of gel (re)moistening and (re)swelling and which both strongly affect the applicability of the materials, dynamic water vapor sorption (DVS) experiments were carried out. Additional information, for example, monolayer moisture load and constants corresponding to monolayer and multilayer sorption energies, was extracted from sorption data, which were fitted to the BET and GAB model.

2. MATERIALS AND METHODS

2.1. Preparation of Lignin Hydrogels and Xerogels. Spruce organosolv lignin (OSL) (Organocell lignin; NaOH/MeOH/anthraquinone [AQ] pulping) precipitated with sulphuric acid at pH 4 was obtained from the former Organocell Co., Munich, Germany. Hydrogen peroxide was purchased from Merck, Darmstadt, Germany, and Poly(ethylene) glycol diglycidyl ether (M_w 526 g mol^{-1}) from Sigma Aldrich, Steinheim, Germany.

2.1.1. Preoxidation of OSL. This was accomplished with H_2O_2 in alkaline media: 5 g of lignin was dissolved in 8 mL of 3.3 mol L^{-1} NaOH at ambient temperature. After 24 h of stirring, 1 mL of H_2O_2 (5%, v/v) was added dropwise, and the mixture was stirred for another 24 h.

2.2.2. Cross-Linking of Preoxidized OSL. This was performed with PEGDGE (Scheme 1) by adding 0.5 mmol, 0.78 mmol, or 1.0 mmol PEGDGE g_{lig}^{-1} immediately after oxidative treatment.[16,19] The reaction mixture was stirred until its viscosity drastically increased through gel formation and was subsequently allowed to rest for at least 24 h. The gels were thoroughly washed, neutralized with deionized water and transformed into xerogels by lyophilization as described

Scheme 1. Reaction Scheme for PEGDGE-Mediated Cross-Linking of Phenolic Substructures of Lignin and Formation of Oligo(oxyethylene) Lignin[16,19]

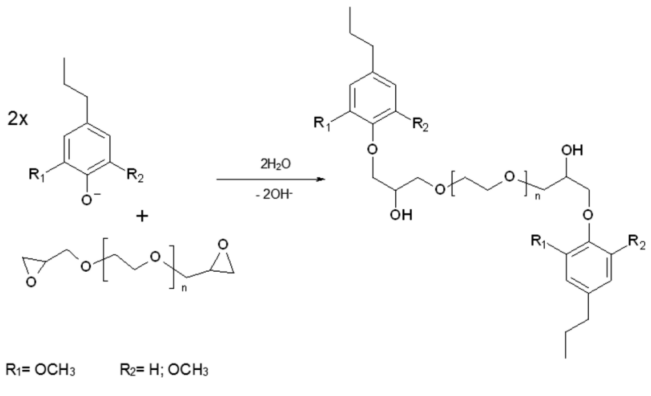

dx.doi.org/10.1021/am3015179 | ACS Appl. Mater. Interfaces 2012, 4, 5852−5862

previously.[18] For analytical purposes, xerogel samples were pestled. The reaction products are referred to as oligo(oxyethylene) lignins ($OOEL_{0.5}$, $OOEL_{0.78}$, and $OOEL_{1.0}$).[16]

2.2. Characterization of OOEL Gels. *2.2.1. Fourier Transformed Infrared Spectroscopy.* ATR FTIR spectra of OSL and xerogel samples were recorded with a Nicolet iS5MIR FTIR spectrometer equipped with a deuterated triglycin sulfate detector using the ATR accessory kit id5. The spectra were measured from 4000−500 cm^{-1} (spectral resolution: 4 cm^{-1}; 32 scans per spectrum). Baseline correction and vector-normalization of spectra was carried out using Bruker's OPUS V.6 software. Further data analysis and graphical spectra representation was by using Origin V 7.5G.

2.2.2. Phenolic Hydroxyl Group Content. OH_{phen} of OSL and OOEL variants were determined by selective aminolysis of per-acetylated samples with pyrrolidine (Scheme 2b) and quantification of

Scheme 2. (a) Acetylation of Lignin Structures with Acetic Anhydride in Pyridine;[32] (b) Selective Aminolysis of Phenylacetates with Pyrrolidine in Dioxane and Formation of 1-Acetyl Pyrrolidine[31]

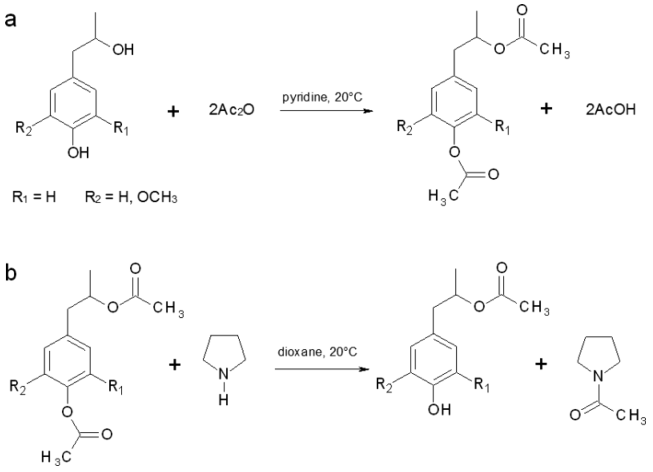

the resulting 1-acetyl pyrrolidine by GC;[31] GC conditions: GC/FID autosystem Perkin-Elmer; column, ROTICAP - 5 MS; temperature program, 160 °C, 4 min; injector, 230 °C; detector, 260 °C; carrier gas, He, 2 mL min^{-1}; combustion gas, H_2, 30 mL min^{-1} and synthetic air, 310 mL min^{-1}. The GC system was calibrated with 1-acetyl pyrrolidine AP (FRINTON Laboratories Inc.) and propionyl pyrrolidine. Chromatograms were analyzed with TotalChrom Workstation V. 6.3.1. Acetylation of parent and PEGDGE-modified lignin was accomplished with acetic anhydride in pyridine (Scheme 2a) according to Glasser and Jain.[32]

2.2.3. Free Swelling Capacity. FSC of lignin hydrogels was calculated from the amount of deionized water (g_{H2O} g_{XG}^{-1}) a xerogel can absorb and retain against gravitation in fully swollen state by FSC = (m_{HG} − m_{XG})/ m_{XG} with m_{XG} (g) being the solids mass of the swollen hydrogel (determined by drying at 105 °C) or the mass of the xerogel, and m_{HG} (g) the mass of the swollen hydrogel. Total water content M_{TW} (%, w/w) was calculated from triplicate measurements by $M_{TW} = 1 - (m_{XG}/m_{HG})$.

2.2.4. Free and Bound Water. Determination of M_{FW} and M_{BW} in OOEL hydrogels was conducted in triplicate using a Mettler-Toledo DSC 821^e. Water saturated gels were transferred into 40 μL hermetic aluminum crucibles which were tightly sealed with aluminum lids to prevent water loss during thermal scanning (−50 to 50 °C; heating rate, 10 K min^{-1}; purge gas, air; flow rate, 15 mL min^{-1}). The phase transition of free water in the hydrogels during heating was recorded as endothermic peak which was integrated using STAR^e V. 9.2 software. The corresponding enthalpies were determined using baseline-corrected and weigth-normalized thermograms. The bound water fraction (% w/w) was calculated as $M_{BW} = M_{TW} - Q_{endo}/Q_f$ with Q_{endo} (J g^{-1}) being the specific heat of fusion of freezable (bulk) water in hydrogels obtained from DSC thermograms, and Q_f the specific heat of fusion of pure water (333 J g^{-1}).[33] M_{FW} (%, w/w) is obtained by subtracting M_{BW} from M_{TW}.

2.2.5. Scanning Electron Microscopy. SEM images of the surface of OSL and xerogel samples were obtained using a JEOL T330A, operating at 15 kV acceleration voltage. For SEM analysis, dried xerogel samples were double-coated by vaporizing their surface with a 40 nm carbon layer under high vacuum (vaporizing unit Emitech K950 carbon coater) and finally sputter-coated with a 30 nm gold layer (ion sputter JEOL JFC 1100E).

2.2.6. Dynamic Vapor Sorption Analysis. DVS was performed in duplicate using a TA Instruments Q5000 SA dynamic vapor sorption analyzer. RH in the sample chamber is adjusted by mixing streams of dry and moist nitrogen which continuously flow around the sample. Operating temperature was set to 25 °C, and a stepwise RH increment was programmed. OSL and OOEL xerogels were preconditioned in a desiccator over P_2O_5 for 10 days. Once ∼5 mg of sample was loaded, 0% RH was maintained until the relative change in sample mass remained below 0.001% within 5 min. The measurement protocol involved three cycles (Figure 1a): a stepwise adsorption from 0% RH

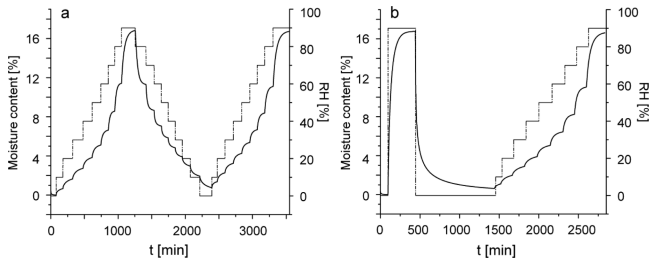

Figure 1. Stepwise increase and decrease in RH after (a) preconditioning at RH = 0% and (b) after preconditioning at RH = 90%, subsequently at RH = 0%. The resulting moisture uptake response is of xerogel $OOEL_{1.0}$.

to 90% RH ($Ad1_{0\%}$) followed by a stepwise desorption to 0% RH ($De1_{0\%}$). Step interval was 10% RH. Finally, a second stepwise adsorption was conducted ($Ad2_{0\%}$). At each RH, equilibration was stopped when the relative change in sample mass (microbalance sensitivity: < 1 μg) was <0.01% for 5 min, and the subsequent RH was automatically adjusted. A second measurement protocol comprised a single-step increase of RH from 0 to 90%, a subsequent single-step decrease of RH to 0% and, finally, the stepwise adsorption from 0% to 90% RH at 10% intervals ($Ad1_{90\%}$; Figure 1b).

2.2.7. BET Model Fitting. Sorption isotherms were fitted to the BET equation to express equilibrium moisture load per unit dry matter M_{eq} (mg g^{-1})

$$M_{eq} = \frac{M_0 C_b a_w}{(1 - a_w)(1 + [C_b - 1]a_w)} \quad (1)$$

with a_w is the given *RH* expressed as water activity, M_0 the monolayer moisture load (mg g^{-1}), and C_b the BET monolayer energy constant. To calculate BET parameters, we rearranged eq 1 to a linear polynomial in terms of a_w as suggested by Timmermann et al.[34]

$$\frac{a_w}{(1 - a_w)M_{eq}} = \alpha + \beta a_w \quad (2)$$

with $\alpha = 1/(M_0 - C_b)$ and $\beta = 1/(C_b - 1)/(M_0 C_b)$. Least-squares regression of eq 2 was performed for $0.1 < a_w < 0.4$. M_0 and C_b were computed from intercept α and gradient β by $1/(\alpha + \beta)$ and $(\alpha + \beta)/\alpha$, respectively.[34]

2.2.8. Specific Surface Area. The correlation between experimental and modeled data for $a_w < 0.4$ allows the determination of the specific surface $A_{BET,\ H2O}$ (m^2 g^{-1}) by

$$A_{BET_{H_2O}} = \frac{M_0 N_0 a_m}{M_{sorb}} \quad (3)$$

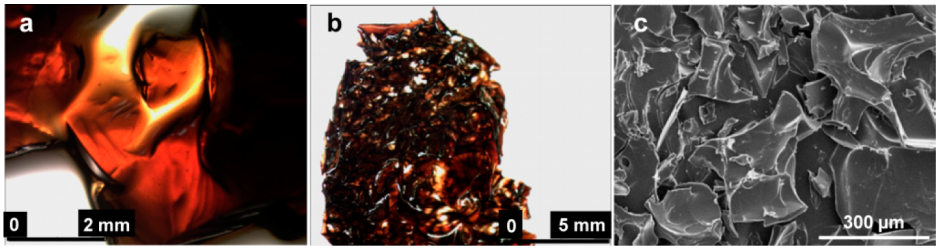

Figure 2. Microscopic images of (a) a swollen $OOEL_{0.5}$ hydrogel particle, (b) the freeze-dried xerogel counterpart with glassy structure, and (c) the corresponding crushed xerogel.

Table 1. Phenolic Hydroxyl Contents (OH_{phen}) of OSL and OOEL Xerogels, Free Swelling Capacities (FSC), Total Water Content (M_{TW}), and Loads of Free (M_{FW}) and Bound (M_{BW}) Water on the Corresponding Water-Saturated OOEL Hydrogels

sample	OH_{phen} (%)	FSC (g_{H2O} g_{XG}^{-1})	M_{TW} (%)	M_{FW} (g_{H2O} g_{XG}^{-1})	M_{BW} (g_{H2O} g_{XG}^{-1})
OSL	6.55	1.70[a]			
$OOEL_{0.5}$	3.01	76.56	98.71	76.19	0.37
$OOEL_{0.78}$	2.38	19.80	95.19	18.84	0.96
$OOEL_{1.0}$	1.83	16.10	94.15	14.63	1.47

[a]Water retention value (g_{H2O} g_{Lig}^{-1}).

with a_m being the area captured by a single water molecule at sorbent surface (i.e., 1.06×10^{-19} m^2 per molecule at 25 °C,[35]), N_0 the Avogadro constant (6.022×10^{23} molecules mol^{-1}), and M_{sorb} the molecular mass of the sorbate (18 g mol^{-1}).

2.2.9. GAB Model. The GAB model extends eq 1

$$M_{eq} = \frac{M_0 C_g k_g a_w}{(1 - k_g a_w)(1 + [C_g - 1]k_g a_w)} \quad (4)$$

with C_g and k_g the characteristic constants for GAB monolayer and multilayer sorption energy, respectively. To calculate GAB parameters, eq 4 was rearranged[34]

$$\frac{a_w}{M_{eq}} = \alpha a_w^{\,2} + \beta a_w + \gamma \quad (5)$$

with $\alpha = k_g(1 - C_g)/M_0C_g$, $\beta = (C_g - 2)/(M_0C_g)$, and $\gamma = 1/(M_0C_gk_g)$. Coefficients α, β, and γ were obtained by least-squares regression of eq 5, and GAB parameters M_0, k_g, and C_g were obtained from the corresponding expressions.[25]

2.2.10. Statistical Analysis. The quality of the fits was estimated by the coefficient of determination (R^2). As a measure of the experimental dispersion of sorption data in BET and GAB models, we applied the normalized error function (NEF), which is the root-mean-square error (RMSE) adjusted for monolayer capacity.[34]

3. RESULTS AND DISCUSSION

3.1. Chemical Characterization and Swelling Properties. Chemical modification and cross-linking of H_2O_2-preactivated OSL resulted in hydrogels (Figure 2) with FSC up to 76.6 g_{H2O} g_{XG}^{-1} (Table 1).

Similar to hydrogels based on PEGDGE-modified kraft lignin Indulin AT, FSC depends on the amount of PEGDGE used for cross-linking.[16] $OOEL_{0.78}$ and $OOEL_{1.0}$ had a significantly lower FSC of 19.8 and 16.1 g_{H2O} g_{XG}^{-1}, respectively, because of the increased cross-linking density and the formation of more closely meshed chemical networks with a smaller pore volume. In such gels, the osmotically driven swelling and polymer expansion is counteracted by a large number of molecular cross-junctions and entanglements leading to increased polymer−polymer interactions.[36]

Total, free, and bound water are specified as moisture load per unit dry substance (g_{H2O} g_{XG}^{-1}), or as fraction of the total mass of the swollen hydrogel (%, w/w). Bound water in OOEL hydrogels (Table 1) increases with increasing degree of etherification from 0.37 ($OOEL_{0.5}$) to 1.47 g_{H2O} g_{XG}^{-1} ($OOEL_{1.0}$), which corresponds to a relative moisture of 0.48 and 8.60%, respectively. Generally, the bound water fraction in hydrogels can exist in the following categories: (1) polarized around charged ionic groups; (2) oriented around hydrogen binding groups and dipoles;[37] that is, both hydrophilic ether O atoms and secondary OH groups of the oligo(oxyethylene) (OOE) substituents in PEGDGE-modified lignin gels (Scheme 1). Because lignin possesses a comparatively low content of charged ionic groups, e.g., carboxyl groups, these functionalities play only a minor role in that of gel swelling. The disappearance of the carboxylic acid C═O stretching vibration υ(C═O) in the ATR FTIR spectrum of $OOEL_{0.5}$ (Figure 3b, left) which is clearly detectable in the spectrum of parent OSL (Figure 3a, left) at 1710 cm^{-1}, suggests the conversion into the corresponding sodium acetates[38] that were formed during gel synthesis in NaOH, resulting in a decrease of charged carboxylate ions. Hence, their potential contribution to swelling

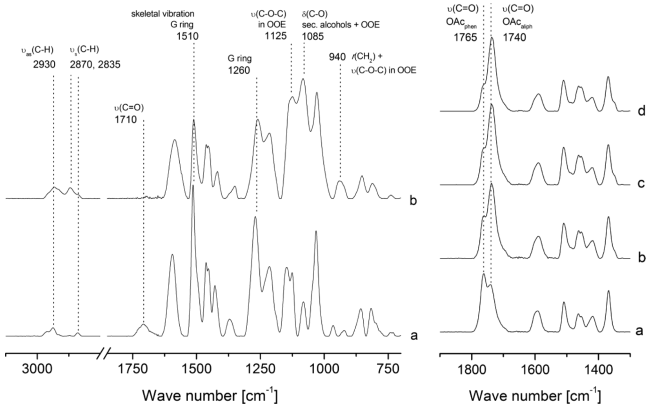

Figure 3. ATR FTIR spectra of (a) OSL and (b) xerogel variant $OOEL_{0.5}$; G, guajacyl units; OOE, oligo(oxyethylene) substituent (left) and zoom into the region between 1800 and 1300 cm^{-1} of per-acetylated counterparts (right) of (a) OSL, (b) $OOEL_{0.5}$, (c) $OOEL_{0.78}$, and (d) $OOEL_{1.0}$.

dx.doi.org/10.1021/am3015179 | ACS Appl. Mater. Interfaces 2012, 4, 5852−5862

because of charge repulsion (polyelectrolyte effect) and polymer expansion is diminished.

Corresponding to FSC, free water which was determined by integrating the DSC melting peak[40] of water of saturated hydrogels (Figure 4), decreased with increasing cross-linking of

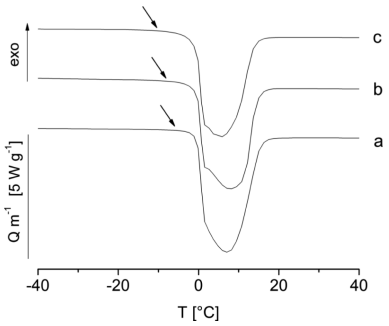

Figure 4. Differential thermograms of hydrogel variants (a) $OOEL_{0.5}$, (b) $OOEL_{0.78}$, and (c) $OOEL_{1.0}$; arrows indicate onset temperature of melting.

the gels. Because bulk water is solely imbibed in capillary pores, this clearly indicates that stronger cross-linked gels possess smaller pore volumes in the swollen state than the slightly cross-linked counterparts. Furthermore, higher cross-linking densities increase polymer−polymer interactions and elastic forces, which counteract the osmotically driven polymer expansion and are therefore accompanied with reduced polymer−solvent interactions and swelling inhibition.[36] This is in line with observations concerning the impact of cross-linking on FSC of hydrogels, which comprise both free and bound water. The shift in the melting peak onset to lower temperature indicates a higher content of intermediate water in stronger cross-linked gels (Figure 4). This fraction in hydrogels forms icelike cages around hydrophobic domains or functionalities (e.g., aromatic rings in OOEL) and ranges between free and bound water.[33]

Chemical modification and cross-linking of lignin with PEGDGE is reflected by a decreasing content of OH_{phen} (Table 1) as an indicator for the etherification of phenolic substructures of lignin (Scheme 1). Depending on PEGDGE amount, OH_{phen} of cross-linked OOEL xerogels range between 1.83 and 3.01, meaning that 55−72% of the initial phenolic hydroxyls of parent OSL (6.55% OH_{phen}) were etherified with PEGDGE.

In the ATR FTIR spectrum of xerogel $OOEL_{0.5}$ (Figure 3b, left), the appearance of intense bands at 1125 and 1085 cm^{-1} that were assigned to υ(C−O−C) and δ(C−O), respectively, points to the PEDGGE-mediated introduction of OOE substituents $(-CH_2-CH_2-O-)_n$ into the lignin macromolecule. This is supported by increased intensities of the bands at 2930, 2870, and 2835 cm^{-1}, which are related to υ_{as}(C−H) and υ_s(C−H) of methylene groups in OOE. The decreased intensities in the signals at 1510 (C=C skeletal vibration of aromatic rings), 1260 (C−O stretching of phenols), and 815 cm^{-1} (C−H out-of-plane deformation vibration of aromatic rings) which are typical for nonetherified guajacyl (G) units[39] also serve as indicators for the etherification of G units and, thus, cross-linking of these structures with PEGDGE.[19]

This finding is supported by the ATR spectra of acetylated lignin and xerogel counterparts (Figure 3, right). The decreasing intensity of the band at 1765 cm^{-1}, assigned to υ(C=O) of aromatic acetoxy groups, and the increasing strength of υ(C=O) at 1740 cm^{-1} for aliphatic acetoxy groups,[40] with an increasing amount of PEGDGE clearly indicate the etherification of phenolic substructures with PEGDGE, which is linked to the formation of new aliphatic hydroxyls because of the ring-opening of the epoxide.[19]

3.2. Sorption Characteristics of OSL. The adsorption and desorption isotherms have a sigmoidal shape (Figure 5a),

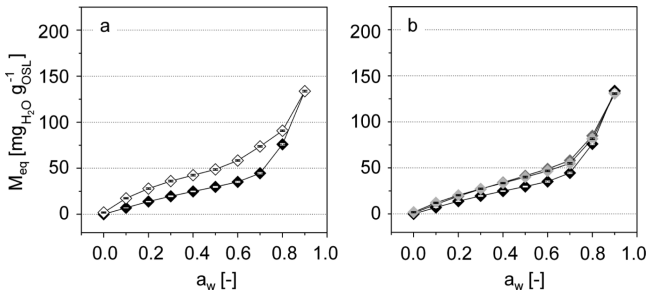

Figure 5. (a) Adsorption (♦) and desorption isotherms (◊) of OSL ($Ad1_{0\%}$, $De1_{0\%}$) and (b) comparison of adsorption isotherms of OSL after preconditioning at 0% RH (♦, $Ad1_{0\%}$; light gray diamond, $Ad2_{0\%}$) and 90% RH (dark gray diamond, $Ad1_{90\%}$).

representing Type II according to Brunauer's classification,[23,41] and are typical for nonporous or macroporous adsorbents with unrestricted monolayer-multilayer adsorption.[30] The results are in accordance with those obtained for different lignins by other authors.[42,43] Chirkova and co-workers[43] connected water vapor sorption of lignin to the globular shape of its primary particles as well as to the aggregates formed thereof (Figure 6).

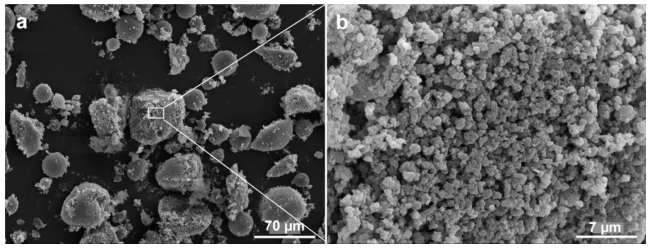

Figure 6. SEM-micrographs of OSL (a) spherical aggregates and (b) primary globular particles.

In such materials, porosity is the result of contacts between spherical globules, and pore size depends on globule size and the number of their contacts. The pores are cavities with narrow necks at contact sites. Physical moisture sorption in such porous and globular structures is mainly caused by vapor condensation. The filling of pores at higher a_w[23] leads to the formation of concave menisci (first, funicular bridges as intermediate state of interstitial liquid) and, finally, to capillary bridges,[22] manifested as a comparatively sharp increase of OSL moisture content at $0.7 \leq a_w \leq 0.9$ (Figure 5a). At low a_w, the interaction of OSL with moisture is weak and, probably, mostly pendular bridges are formed.[22] At $a_w \approx 0.2$, the onset of a linear part of the isotherm is evident, which indicates a stage at which monolayer coverage is completed and multilayer adsorption starts.[30] Moisture sorption of lignin with its predominantly aromatic and therefore hydrophobic properties is associated with hydrophilic functional groups[43] and may be attributed to

hydrogen bonds formed between water molecules and phenolic or aliphatic hydroxyls (OSL contains 6.55% OH_{phen} and 4.52% OH_{aliph}[41]), carboxyl groups (6.37% COOH[41]) and ether O-atoms of methoxyl groups (14% OCH_3[41]), but also between water and α/ β-O-4-ether structures as main linkages between C_9 units in lignin (55−65/100 C_9[3]). Hill and co-workers[44] showed that particularly OH accessibility and the OH/C ratio significantly affect moisture sorption of cellulosics and lignocellulosics, which should also apply to lignin and lignin-based materials.

At any given a_w, higher amounts of water vapor were retained in OSL during desorption so that sorption hysteresis[23] is evident. A similar phenomenon was observed after comparing the $Ad1_{0\%}$ with the $Ad2_{0\%}$ adsorption isotherm. Higher adsorption was also achieved experimentally after a one-step *RH* increase (0−90%) and subsequent one-step decrement back to RH = 0% ($Ad1_{90\%}$; Figure 5b).

3.3. Sorption Characteristics of OOEL Xerogels. Figure 7 depicts $Ad1_{0\%}$ and $De1_{0\%}$ isotherms of OSL modified with 0.5, 0.78, or 1.0 mmol PEGDGE g_{Lig}^{-1}.

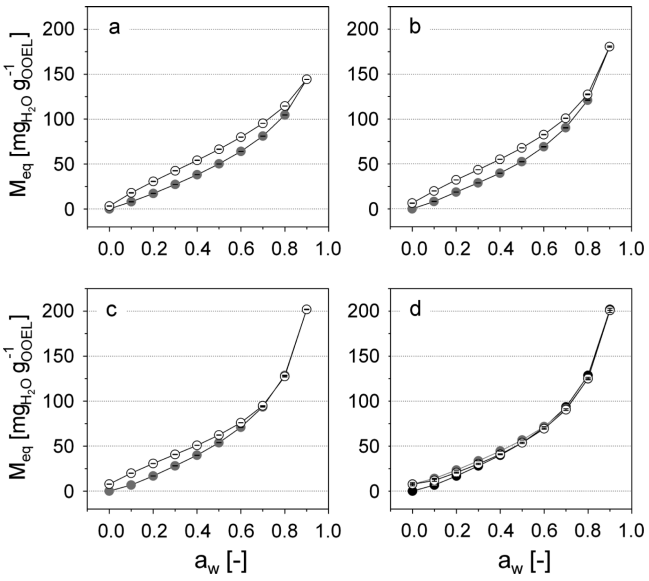

Figure 7. Adsorption (gray circle, $Ad1_{0\%}$) and desorption (○ $De1_{0\%}$) isotherms of xerogel variants (a) $OOEL_{0.5}$, (b) $OOEL_{0.78}$, and (c) $OOEL_{1.0}$; (d) adsorption isotherms of $OOEL_{1.0}$ after preconditioning at 0% *RH* (● $Ad1_{0\%}$; and gray circle, $Ad2_{0\%}$) and 90% *RH* (○ $Ad1_{90\%}$).

Compared to OSL, the a_w-specific water vapor uptake of cross-linked OOEL is higher. This is caused by the sorption of water onto OOE substituents of PEGDGE-modified lignin xerogels, possessing not only hydrophilic ether-O atoms but also primary and secondary OH groups, which additionally increase hydrophilic properties. The differences between OSL and OOEL in moisture sorption at $a_w \leq 0.2$ are, however, comparatively low, meaning that potential adsorption sites of modified lignin are not accessible in the low a_w region.

At intermediate and high vapor pressure, sorption isotherms of OOEL show a more convex increase, which is typical for Type III isotherms.[41] The latter are typical for weak moisture−solid interactions at low a_w and for nonporous and macroporous materials,[23] pointing to the amorphous and glassy character of OOEL. The weakness of adsorbent−adsorbate forces causes the uptake at low a_w to be small. Once a water molecule is adsorbed, the adsorbate−adsorbate forces promote the adsorption of further molecules so that the isotherms become convex.[23,30] In the case of OOEL, this may be caused by the formation of molecular multilayers of water due to the hydration of hydrophilic OOE substituents, which further promote capillary condensation. At this stage of moisture sorption, water molecules penetrate through the lignin xerogel particle surface and water is absorbed once diffusional forces exceed binding forces. Such effects indicate that moisture is capable of altering the structure of OOEL or OOE domains either by plasticization effects where polymers relax,[24] or obscured polar sites (hydroxyl and ether groups) were unfold and available for moisture uptake. Therefore, moisture sorption of modified lignin corresponds well to the degree of chemical modification and points to a strong influence of OOE substituents. The increase in moisture sorption at high a_w is most likely due to a progression of molecular mobility as a consequence of moisture-induced plasticization, which allows the material to swell and indicates a conversion from a glassy (rigid) into a rubbery (elastic) state.[24,25,45] For OOEL xerogels this effect is enlarged with an increasing amount of PEGDGE ($OOEL_{0.5}$ < $OOEL_{0.78}$ < $OOEL_{1.0}$) and corresponds well to the PEGDGE-dependent content of bound water adsorbed during gel swelling. Another explanation for the exponential increase of M_{eq} at high a_w is the formation of heterogeneous gel−water networks or nonideal gel domains.[46] In our case, a nonideal OOEL gel is composed of chemically cross-linked lignin provided with loose chains or chain ends of hydrophilic OOE glycol (OOEG) substituents (Figure 8) grafted on lignin

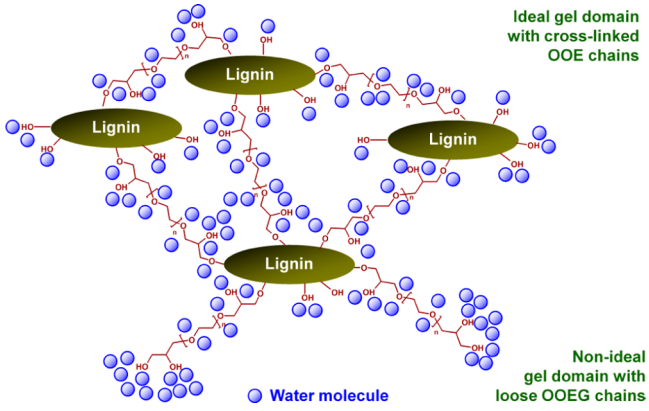

Figure 8. Schematic representation of an OOEL gel with cross-linked OOE chains (ideal gel domain) and domains with loose OOEG chains, grafted on lignin molecules (nonideal gel domain).

molecules, which are probably not involved in intermolecular interactions. Because of predominant contributions from mixing entropy these more or less free OOEG chains may enter solution with adsorbed water and cause the sharp increase of M_{eq} at a_w > 0.80 (Figure 7b, c). This two-phase structural model might be an explanation for the more lignin-like sorption behavior of OOEL xerogels at low a_w and a more OOE/OOEG-like moisture sorption at high a_w, which is typical for materials with strong hydrophilic or water-soluble constituents.[29]

3.4. Interpretation of Moisture Uptake and Sorption Hysteresis. A characteristic feature of water vapor sorption of OSL and OOEL is the occurrence of hysteresis (Figures 5a and 7). Panels a and b in Figure 9 depict absolute hysteresis $h = M_{eq,De1,0\%} - M_{eq,Ad1,0\%}$ and relative hysteresis $dh = (h/M_{eq,Ad1,0\%}) \times 100\%$).[25,43]

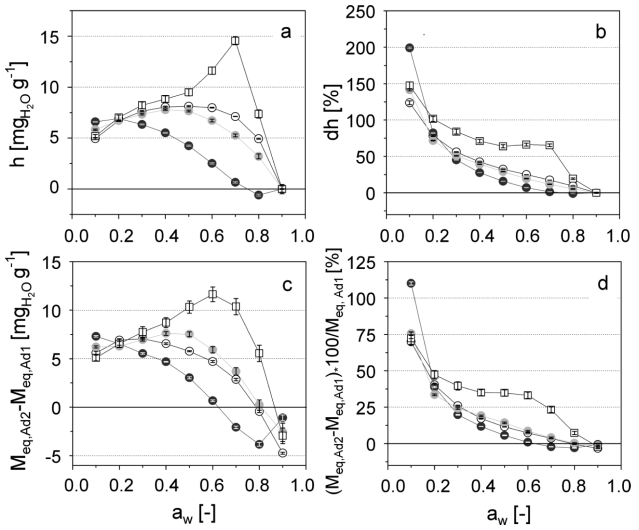

Figure 9. (a) Hysteresis *h*, (b) degree of hysteresis *dh*, (c) absolute and (d) relative deviation of $M_{eq,Ad2,0\%}$ and $M_{eq,Ad1,0\%}$ of OSL (□) and xerogels $OOEL_{0.5}$ (○), $OOEL_{0.78}$ (gray circle), and $OOEL_{1.0}$ (●).

Sorption hysteresis in rigid sorbents such as lignin can be attributed to the irreversible deformation of the sorbent molecules during adsorption,[43] initially described by Tvardovski et al.[47] for clay minerals and also discussed for aromatic compounds such as humic acids.[48] This swelling—connected with the cleavage of weaker interstructural bonds of lignin formed by hydrophobic interactions and hydrogen bonds[49]—precedes diffusion, which continues into newly formed pores in the sorbent[43] and is additionally enforced because of the thermal motion of the sorbate.[50]

Another explanation connects sorption hysteresis with the formation of metastable states of the adsorbate in pores, i.e., capillary condensation in mesopores[23] in the region of intermediate and high a_w. In the presence of concave menisci formed in porous systems, moisture tension affects the pore walls (bottleneck-effect). As a result, the pore walls become sealed blocking the complete release of the sorbate.[43]

The aforementioned facts can also be considered as reasons for a higher M_{eq} at any a_w after subjecting lignin to repeated adsorption ($Ad2_{0\%}$), or after preconditioning at 90% RH ($Ad1_{90\%}$) (Figure 5b). Figures 9c and d reveal that the course of the absolute (= $[M_{eq,Ad2,0\%} - M_{eq,Ad1,0\%}]$) and relative difference function (= $[(M_{eq,Ad2,0\%} - M_{eq,Ad1,0\%}) \times 100/M_{eq,Ad1,0\%}]$) is similar to those of *h* and *dh*, respectively (Figure 9a, b), but the values are considerably lower (approximately 50% of the latter). For OSL, $M_{eq,Ad2,0\%} - M_{eq,Ad1,0\%}$ was highest at $a_w \approx 0.5-0.7$ and then decreased abruptly, reaching negative values at $a_w = 0.9$. Increased differences between $Ad2_{0\%}$ and $Ad1_{0\%}$ up to $a_w = 0.6$ may be explained by moisture entrapment, i.e., remnants of adsorbed moisture after desorption, leading to an increased pore volume compared to the initial pore volume of never-moistened matrices. When the maximum at $a_w = 0.6$ is reached, elastic forces of the polymer exceed diffusional forces, and $M_{eq,Ad2,0\%}$ starts to converge against $M_{eq,Ad1,0\%}$ at high a_w ($\approx 0.7-0.9$).

Higher amounts of moisture were retained during $De1_{0\%}$ and $Ad2_{0\%}$ over the whole a_w range than were acquired during $Ad1_{0\%}$ for all OOEL samples (Figure 9a, b). Contradictory to OSL, hysteresis and deviations between successive adsorption cycles are much lower at high a_w (Figure 7b, c), which was reported as typical for aggregates of platelike particles (Figure 2c) giving rise to slit-shaped pores.[29] From a molecular point of view, this phenomenon indicates a more rubbery character of OOEL networks mediated by plasticizing OOE substituents at high a_w. Polymer shrinkage during desorption induces kinetic barriers to moisture migration, which might explain the moderate differences in M_{eq} between sorption and desorption.[25,47] This molecular rearrangement at low a_w is presumably due to the formation of intermolecular hydrogen bonds between adjacent OOE substituents,[51] and between OOE and phenolic substructures[52] of OOEL, from which adsorbed water molecules are successively liberated during desorption. Therefore, they approach, particularly at low a_w, and interact with each other. For xerogels, highest dh and $(M_{eq,Ad2,0\%} - M_{eq,Ad1,0\%}) \times 100/M_{eq,Ad1,0\%}$ at $a_w \leq 0.2$ are thought to arise from swelling of the adsorbent which increases initial surface area if the deformed structure does not relax.[53] Negative values of $M_{eq,Ad2,0\%} - M_{eq,Ad1,0\%}$ (Figure 9c) could be caused by diminished moisture entrapment effects at high a_w levels:[25] In the wet state (during $Ad1_{0\%}$), hydrophilic groups of OSL and OOEL are almost entirely occupied by sorbed water molecules. During desorption, these groups are freed and draw closer to form hydrogen bonds with each other. Thus, the void fraction of the matrices is probably irreversible reduced and $M_{eqAd2,0\%}$ values are significantly lower than $M_{eq,Ad1,0\%}$. Furthermore, low-pressure hysteresis is indicative (1) for microporous systems[33] and (2) for intense enthalpy changes[25] because of strong and irreversible chemical interactions[30] between water and lignin derivatives, particularly OOE substituents, and corresponds to the degree of lignin cross-linking ($OOEL_{0.5} < OOEL_{0.78} < OOEL_{1.0}$). This is in accordance with sorption characteristics of humic acids for which increasing cross-linking density and molecular mass were found to increase sorption hysteresis because of a diminished flexibility of the macromolecules.[48] During desorption, OOEL is transformed from the rubbery (flexible OOE chains) into the glassy state again (rigid OOE chains), which probably prevents complete molecular refolding from a swollen to a completely reswollen state due to the molecular stiffness at low a_w. Consequently, larger pore volumes remain after desorption, and adsorbate−adsorbent interactions increase and lead to higher M_{eq} than achieved after $Ad1_{0\%}$.

Lower *dh* of $OOEL_{0.5}$ at low a_w indicates a relatively weak specific interaction with water due to the lower content of hydrophilic OOE substituents. For $a_w > 0.5$, slightly ($OOEL_{0.5}$) and moderately PEGDGE-modified lignin ($OOEL_{0.78}$) showed a higher *dh* than $OOEL_{1.0}$, suggesting that the latter is structurally more stable and moisture desorption is not hindered because of changes in polymer confirmation or irreversible deformation. Nevertheless, at $a_w > 0.7$, higher substituted samples adsorb larger amounts of water (Figure 7) caused by plasticization and swelling of OOE substituents with increasing moisture. The absence of hysteresis for highly cross-linked products at $a_w \geq 0.8$ ($OOEL_{0.78}$, $OOEL_{1.0}$) is also an indicator for the rubbery-elastic character of PEGDGE-modified lignin and a low sorption enthalpy at high a_w, both mediated by hydrophilic OOE substituents[54] meaning that water molecules bound as molecular multilayers due to hydration of hydrophilic functional groups are easily desorbed. Furthermore, swelling and shrinkage of OOEL xerogels at high a_w points to a progressive increase of their intrinsic molecular mobility,[24] which might be caused by a gradual decrease in the

glass transition temperature of OOEL gels with increasing moisture.

3.5. BET and GAB Model Fitting. BET and GAB models were fitted to $Ad1_{0\%}$ and $Ad2_{0\%}$ isotherms after sample equilibration at RH = 0%, and to adsorption after equilibration at RH = 90%. Depending on the adsorbent, BET and GAB equations have limits as regards applicability range.[23,29] Appropriate fit limits were therefore identified using the linear (BET) and quadratic (GAB) plot criteria, the latter by considering the inverse-plot method.[34] Figure 10 gives an example of experimental data fitted to these functions (inverse plot not shown).

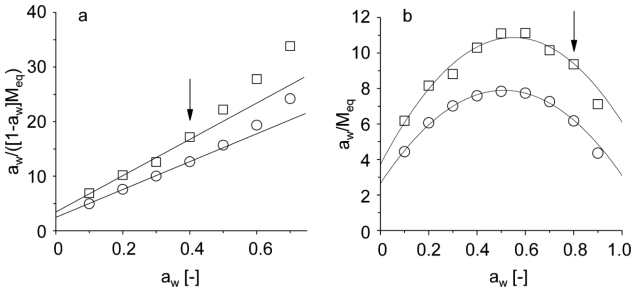

Figure 10. (a) Linear form of BET model and (b) parabolic form of GAB model fitted to the desorption isotherms of OSL (□) and the xerogel $OOEL_{1.0}$ (○); arrows indicate upper fit limits.

Experimental data of $Ad1_{0\%}$ for OSL and OOEL samples show a significant deviation from linear BET and quadratic GAB plots, whereas satisfying fits are evident for $De1_{0\%}$ and $Ad2_{0\%}$ but also for $Ad1_{90\%}$ isotherms in the range of $0.1 \leq a_w \leq 0.4$ (BET) and $0.1 \leq a_w \leq 0.8$ (GAB). BET and GAB parameters were subsequently calculated considering these limits. Nevertheless, it has to be taken into account that fitting of the experimental data causes an overestimation of the sorption for $a_w > 0.4$ (BET), whereas the GAB model slightly underestimates sorption at $a_w > 0.8$ because of the respective model assumptions: The BET model hypothesizes that the energy state of sorbate molecules in second and higher layers is similar to that of the pure liquid. The GAB model improves the BET equation by considering a second sorption stage where the binding energy of the corresponding molecule layer is between that of the monolayer and the pure liquid, but disregards the energy state of liquid water at high a_w.[29]

Table 2 summarizes BET and GAB parameters for $De1_{0\%}$ and $Ad2_{0\%}$ isotherms. R^2 show that the models adequately reflect experimental data in the respective a_w range. The normalized error function, measuring the dispersion of experimental sorption data in the models, is acceptable as long as NEF < 5%.[34] For all samples, NEF for BET fitting are lower than for GAB fitting, indicating that sorption is better represented by the BET model. However, because of the good conformity of BET and GAB parameters, both models will be referred to in further analysis.

In the BET model (eq 1), C_b can be regarded as a measure of the interaction between sorbent surface and water in the monolayer[26]

$$C_b = C\exp\left(\frac{H_0 - H_L}{RT}\right) \quad (6)$$

with constant C, and where H_0 and H_m are the molar heat of sorption in the monolayer and the molar heat of condensation of bulk water, R the universal gas constant, and T the absolute temperature.[26] In the GAB model (eq 4), C_g and k_g are related to the net heat of sorption of the monolayer and multilayer, respectively, so that C_g is a measure of the interaction between the surface of the sorbent and water molecules in the monolayer[26]

$$C_g = C\exp\left(\frac{H_0 - H_m}{RT}\right) \quad (7)$$

and k_g is a measure for the interaction between the sorbent and water molecules in the multilayer

$$k_g = k\exp\left(\frac{H_L - H_m}{RT}\right) \quad (8)$$

with constant k and H_m the molar heat of sorption in multilayers.

The monolayer capacity for OSL obtained from desorption isotherms is 29.53 (BET) and 34.19 mg g^{-1} (GAB) which is in accordance with literature.[42,43] M_0 of OOEL xerogels is 35.68–41.09 mg g^{-1} (BET) and 38.21–58.17 mg g^{-1} (GAB) and

Table 2. BET and GAB Coefficients and Parameters of Fits for $De1_{0\%}$ and $Ad2_{0\%}$ Isotherms of OSL and OOEL Xerogels

	$De1_{0\%}$				$Ad2_{0\%}$			
	OSL	$OOEL_{0.5}$	$OOEL_{0.78}$	$OOEL_{1.0}$	OSL	$OOEL_{0.5}$	$OOEL_{0.78}$	$OOEL_{1.0}$
				BET[a]				
M_0 (mg g^{-1})	29.53	41.09	40.06	35.68	24.47	35.34	37.25	34.57
C_b	11.16	5.87	7.26	8.96	7.59	4.79	4.76	4.95
R^2	0.992	0.999	0.999	0.999	0.995	0.999	0.999	0.996
NEF (%)	2.98	0.78	0.36	0.51	1.83	0.59	0.43	1.01
RMSE (mg g^{-1})	0.88	0.32	0.14	0.18	0.21	0.21	0.16	0.35
A_{BET} (m^2 g^{-1})	96.78	145.71	142.06	126.50	86.78	125.33	132.10	122.60
				GAB[b]				
M_0 (mg g^{-1})	34.19	58.17	49.40	38.21	27.32	48.16	46.46	37.66
C_g	10.82	5.20	6.52	11.66	8.14	4.26	4.30	3.82
k_g	0.80	0.70	0.81	0.90	0.83	0.75	0.83	0.91
R^2	0.982	0.992	0.993	0.996	0.898	0.988	0.978	0.976
NEF (%)	15.77	1.59	7.65	7.62	36.33	3.84	7.80	7.22
RMSE (mg g^{-1})	5.39	0.92	3.78	2.91	9.92	1.85	3.62	2.72

[a]Model range BET: $0.1 \leq a_w \leq 0.4$. [b]GAB: $0.1 \leq a_w \leq 0.8$.

decreases with increasing cross-linking through PEGDGE. The order of M_0 is OSL < $OOEL_{1.0}$ < $OOEL_{0.78}$ < $OOEL_{0.5}$. Despite the strong hydrophilic properties of OOE substituents, lower amounts of water vapor were bound in highly substituted OOEL at low a_w, indicating a decreasing number or lower accessibility of adsorption sites and suggesting strong intermolecular interactions between adjacent OOE substituents or between OOE substituents and phenolic substructures of lignin.[51,52] Therefore, potential hydrophilic adsorption sites are occupied in shrunken OOEL xerogels which is also evident from specific surface area. For parent OSL, A_{BET} = 96.78 m^2 g^{-1} is similar to literature data on organosolv lignins,[43] whereas for PEGDGE-modified variants, A_{BET} decreases with increasing cross-linking from 145.71 to 126.50 m^2 g^{-1}. Although A_{BET} obtained by using water vapor as sorbate is considerably overestimated compared to N_2 sorption data,[30,43] this procedure is often used to obtain specific surface areas of different matrices.[34,43]

C_b and C_g increased with increasing degree of PEGDGE-substitution, suggesting that the driving force for monolayer binding is amplified because of OOE substituents so that physicochemical moisture sorption is increased. As soon as OOE substituents in PEGDGE-modified lignin xerogels become accessible for water molecules at higher a_w because of plasticization and swelling of the gels, they considerably contribute to sorption on the OOEL xerogel surface and to the subsequent formation of multilayers. This is supported by k_g (0.70−0.90). Generally, k_g is related to the chemical potential difference of the pure liquid state and the multilayer water molecules.[29] k_g of xerogels feature a consistent trend $OOEL_{1.0}$ < $OOEL_{0.78}$ < $OOEL_{0.5}$, meaning that aforementioned water vapor interaction effects are limited to the monolayer and do not affect the state of multilayer water (an increase of k_g indicates diminished interactions of water molecules with sorbent surface). k_g increased in the order of $OOEL_{0.5}$ < $OOEL_{0.78}$ < $OOEL_{1.0}$ which indicates that second stage or multilayer sorption is higher because of OOE substituents. k_g do also coincide with the distinct upward curvature of isotherms at high a_w (Figure 7).[29]

M_0 from $Ad2_{0\%}$ isotherms is generally lower. In line with lower C_b and C_g, this points to weaker forces for monolayer binding during adsorption. Lower heat of adsorption as compared to desorption may be an indicator for structural modifications taking place at adsorbent surface during sorption which modify the binding energy of moisture by, e.g., deformation of sorbent molecules during adsorption,[47] entrapment effects during desorption,[25] or cooperative binding or adsorbate−adsorbate interactions.[23,30] Desorption C_g which were higher by a factor of 1.33, 1.22, 1.52, and 3.03 for OSL, $OOEL_{0.5}$, $OOEL_{0.78}$, and $OOEL_{1.0}$, respectively, and which were, in contrast to adsorption, inversely related to M_0 for xerogel variants also imply that adsorbed moisture changes the physicochemical nature of lignin and lignin xerogel surface. As a result, the binding stability of the monolayer and the number of hydrophilic sites increases. The extent of these structural changes strongly depends on the content of hydrophilic OOE substituents in xerogel variants and increases with OOE content.

Model parameters obtained by fitting adsorption isotherms $Ad1_{90\%}$ of selected samples are summarized in Table 3.

For OSL, M_0 from BET and GAB fitting is slightly higher than M_0 calculated from the $Ad2_{0\%}$ isotherm, whereas the inverse is true for $OOEL_{1.0}$ (Table 2). C_b and C_g are lower by

Table 3. BET and GAB Coefficients and Fit Parameters for $Ad1_{90\%}$ Isotherms of OSL and $OOEL_{1.0}$

	$Ad1_{90\%}$	
	OSL	$OOEL_{1.0}$
	BET[a]	
M_0 (mg g^{-1})	27.11	34.03
C_b	4.995	3.86
R^2	0.989	0.997
NEF (%)	1.88	0.65
RMSE (mg g^{-1})	0.05	0.22
A_{BET} (m^2 g^{-1})	96.14	120.68
	GAB[b]	
M_0 (mg g^{-1})	28.18	38.43
C_g	5.97	3.65
k_g	0.863	0.908
R^2	0.805	0.996
NEF (%)	15.08	3.28
RMSE (mg g^{-1})	4.25	1.26

[a]Model range BET: $0.1 \le a_w \le 0.4$; [b]GAB: $0.1 \le a_w \le 0.8$

the factors of 1.52 (BET) and 1.36 (GAB), and by 1.28 (BET) and 1.05 (GAB) for OSL and $OOEL_{1.0}$, respectively, pointing to reduced monolayer binding forces. This also applies to multilayer water in lignin, indicated by an increase of k_g. Obviously, preconditioning at RH = 90% increases the accessibility of lignin surface for water vapor, probably because of a preswelling leading to irreversible deformation of the molecular network and the formation of new capillaries and pores,[43] which allows the material to subsequently adsorb larger amounts of moisture. The reduced monolayer sorption capacity for the xerogel counterpart may be explained by a structural concealment of potential sorption centers during rapid one-step desorption at RH = 0%, connected with irreversible shrinking of premoistened material and a local collapse of micropores. Chemically, this phenomenon is induced by OOE substituents of PEGDGE-modified lignin, which were abruptly freed during this desorption. Subsequently, adjacent OOE/OOEG chains interact with each other by forming intermolecular hydrogen bonds.[51] $Ad1_{90\%}$ k_g of the xerogel was similar to $Ad2_{0\%}$ k_g (0.908 and 0.910, respectively) meaning that the state of multilayer water is not affected by rapid one-step adsorption and desorption.

4. CONCLUSIONS

A spruce organosolv lignin and PEGDGE-modified freeze-dried xerogel counterparts were analyzed with respect to swelling properties and dynamic moisture sorption characteristics, which were related to the chemical structure and microstructure of the materials. The degree of chemical modification results in a decreasing content of phenolic hydroxyl groups of OOEL xerogels, indicating that lignin derivatization by PEGDGE mainly occurs through etherification of phenolic hydroxyls. Free and bound water in OOEL hydrogels were found to be opposing parameters and are strongly dependent on the degree of PEGDGE-modification of lignin. DVS measurements showed significant differences in moisture sorption characteristics of lignin and modified xerogels, and are mainly related to the globular structure of parent lignin particles and to the OOE content of modified lignin, respectively. The results indicate that increased moisture sorption and swelling of PEGDGE-modified xerogels at high RH are mainly caused by hydration/dissolution as well as plasticization effects, both mediated by

hydrophilic OOE/OOEG substituents. By applying BET and GAB models which were found to be relevant in describing moisture sorption up to a_w = 0.4 (BET) and a_w = 0.8 (GAB) it was found that monolayer sorption of xerogels decreased with increasing degree of PEGDGE-modification and correlates with the swelling capacity of the hydrogels. Contrary, driving forces for monolayer binding are amplified. The state of multilayer water, which was found to be easily desorbable, is unaffected by the degree of chemical modification with PEGDGE, even at comparatively rapid changes in RH. From a materials point of view, (1) the availability of multilayer water, (2) the reswellability of xerogels and retention of water from the vapor phase even after exposing moistened gels to dryness, (3) moderate to high swelling capacities, and (4) the potential role as a precursor for the formation of soil humic substances should render PEGDGE-modified lignin as applicable for different utilization purposes, particularly as water-storing soil conditioner for agriculture, forestry, and soil rehabilitation.

AUTHOR INFORMATION

Corresponding Author

*Tel: +49-351-4662-369. Fax: +49-351-4662-211. E-mail: Lars.Passauer@ihd-dresden.de.

Present Addresses

[§]Institute of Food Chemistry, Leibniz Universitaet Hannover, Hannover, Germany

[#]Department of Energy Process Engineering and Chemical Engineering, Technische Universitaet Bergakademie Freiberg, Freiberg, Germany

Notes

The authors declare no competing financial interest.

ACKNOWLEDGMENTS

The authors thank N. Herold (Eberswalde University of Sustainable Development, Eberswalde, Germany) for the assistance with ATR FTIR spectroscopy, and E. Baeucker and B. Guenther (Department of Forest Sciences, Technische Universitaet Dresden) for recording electron micrographs and light-microscopic images.

REFERENCES

(1) Heitner, C., Dimmel, D., Schmidt., J., Eds. *Lignin and Lignans: Advances in Chemistry*; CRC Press: Boca Raton, FL, 2010.

(2) Freudenberg, K., Neish, A. C. *Constitution and Biosynthesis of Lignin*; Springer: Berlin, 1968.

(3) Sarkanen, K. V., Ludwig, C. H. *Lignin: Occurrence, Formation, Structure and Reactions*; Wiley: New York, 1971.

(4) Funaoka, M. *Macromol. Symp.* **2003**, *201*, 213−221.

(5) Faix, O. *Das Papier* **1992**, *12*, 733−739.

(6) Glasser, W. G., Northey, R. A., Schultz, T. P. *Lignin: Historical, Biological and Materials Perspectives*; ACS Symposium Series; American Chemical Society: Washington, D.C., 2000; Vol. *742*.

(7) Hu, T. Q. *Chemical Modification, Properties and Usage of Lignin*; Kluwer Academic/ Plenum Publishers: New York, 2002.

(8) Brown, W. Process for making lignin gels in bead form. Patent U.S. 4 131 573, December 26, 1978.

(9) Delicolli, H. T., Dillinng, P., Falkehag, S. Cross-linked lignin gels. Patent U.S. 4 244 728, January 13, 1981

(10) Yamamoto, H.; Amaike, M.; Saito, H.; Sano, Y. *Mater. Sci. Eng.* **2000**, *C7*, 143−147.

(11) Lindström, T.; Wallis, A.; Tulonen, J.; Kolseth, P. *Holzforschung* **1988**, *42*, 225−228.

(12) Lindström, T.; Westmann, L. *Colloid Polym. Sci.* **1980**, *258*, 390−397.

(13) El-Zawawy, W. K. *Polym. Adv. Technol.* **2005**, *16*, 48−54.

(14) Nishida, M., Uraki, Y., Sano, Y. Preparation of lignin based hydrogel and its interactions with amphiphilic compounds. *Proceedings of the 11th International Symposium on Wood and Pulp Chemistry*; Nice, France, June 11−14, 2001.

(15) Nishida, M.; Uraki, Y.; Sano, Y. *Bioresour. Technol.* **2003**, *88*, 81−83.

(16) Passauer, L.; Fischer, K.; Liebner, F. *Holzforschung* **2011**, *65*, 309−317.

(17) Passauer, L.; Fischer, K.; Liebner, F. *Holzforschung* **2011**, *65*, 319−326.

(18) Passauer, L., Guenther, B., Baeucker, E. Morphology of highly swellable hydrogels from oligo(oxyethylene) derivatives of lignin. *Proceedings of the 3rd Nordic Wood and Biorefinery Conference*; Stockholm, Sweden, March 22−24, 2011.

(19) Passauer, L. Highly swellable lignin hydrogels − Materials with interesting properties. In *Functional Materials from Renewable Sources*; Rosenau, T., Liebner, F., Eds.; ACS Symposium Series; American Chemical Society: Washington, D.C., 2012; Vol. *1107*, pp 211−228.

(20) Passauer, L., Liebner, F., Fischer, K., Katzur, J. Substrate for soil improvement having water storing property, method for producing same and use thereof. Patent WO 2011, 098078, August 18, 2011

(21) Hayashi, J.; Shoij, T.; Watada, Y.; Muroyama, K. *Langmuir* **1997**, *13*, 4185−4186.

(22) Urso, M. E. D.; Lawrence, C. J.; Adams, M. A. *J. Colloid Interface Sci.* **1999**, *220*, 42−56.

(23) Gregg, S. J., Sing, K. S. W. *Adsorption, Surface Area and Porosity*, 2nd ed.; Academic Press: London, 1982.

(24) Champion, D.; Loupiac, C.; Simatos, D.; Lillford, P.; Cayot, P. *Food Biophys.* **2011**, *6*, 160−169.

(25) Mutungi, C.; Schuldt, S.; Onyango, C.; Schneider, Y.; Jaros, D.; Rohm, H. *Biomacromolecules* **2011**, *12*, 660−671.

(26) Al-Muhtatseb, A. H.; McMinn, W. A. M.; Magee, T. R. A. *Food Bioprod. Proc. (Trans. Inst. Chem. Eng. C)* **2002**, *80*, 118−128.

(27) Reid, D. S. In *Water Activity in Foods. Fundamentals and Applications*. Barbosa-Canovas, G. V., Fontana, A. J., Schmidt, S. J., Labuza, T. B., Eds. Blackwell Publishing: Oxford, U.K., 2007.

(28) Brunauer, S.; Emmett, P. H.; Teller, E. *J. Am. Chem. Soc.* **1938**, *60*, 309−310.

(29) Timmermann, E. O. *Colloids Surf., A* **2003**, *220*, 235−260.

(30) Sing, K. S.; Everett, D. H.; Haul, R. A. W.; Moscou, L.; Pierotti, R. A.; Rouquerol, J.; Siemeniewska, T. *Pure Appl. Chem.* **1985**, *57*, 603−619.

(31) Månsson, P. *Holzforschung* **1983**, *87*, 143−146.

(32) Glasser, W. G.; Jain, K. J. *Holzforschung* **1993**, *47*, 225−233.

(33) Wang, T.; Gunesakaran, G. *J. Appl. Polym. Sci.* **2006**, *101*, 3227−3232.

(34) Timmermann, E. O.; Chirife, J.; Iglesias, H. A. *J. Food Eng.* **2001**, *48*, 19−31.

(35) Arslan, N.; Togrul, H. *J. Stored Prod. Res.* **2006**, *42*, 112−135.

(36) Richter, A.; Paschew, G.; Klatt, S.; Lienig, J.; Arndt, K.-F.; Adler, H.-J. P. *Sensors* **2008**, *8*, 561−581.

(37) Liu, Y.; Huglin, M. B. *Polym. Int.* **1995**, *37*, 63−67.

(38) Zier, N. Structural features of an organosolv lignin under variation of the pulping conditions. *Ph.D. Thesis*, Technische Universitaet Dresden, Dresden, Germany, 1996

(39) Faix, O. *Holzforschung* **1991**, *45*, 21−27.

(40) Faix, O.; Argyropoulos, D.; Robert, D.; Neirinck, V. *Holzforschung* **1994**, *48*, 387−394.

(41) Brunauer, S.; Deming, L. S.; Deming, W. E.; Teller, E. *J. Am. Chem. Soc.* **1940**, *62*, 1723−1732.

(42) Volkova, N.; Ibrahim, V.; Hatti-Kaul, R.; Wadsö, L. *Carbohydr. Polym.* **2012**, *87*, 1817−1821.

(43) Chirkova, J.; Andersons, B.; Andersone, I. *Bioresources* **2007**, *4*, 1044−1057.

(44) Hill, A. S. C.; Norton, A.; Newman, G. *J. Appl. Polym. Sci.* **2009**, *112*, 1524−1537.

(45) Doumenc, F.; Guerrier, B.; Allain, C. *Europhys. Lett.* **2006**, *76*, 630−636.

(46) Li, S.; Tang, J.; Chinachoti, P. *J. Polym. Sci., Part B: Polym. Phys.* **1996**, *34*, 2579−2589.
(47) Tvardovski, A. V.; Fomkin, A. A.; Tarasevich., Y. I.; Zhukova, A. I. *J. Colloid Interface Sci.* **1997**, *191*, 117−119.
(48) Lu, Y.; Pignatello, J.J. J. *Environ. Qual.* **2004**, *33*, 1314−1321.
(49) Roblin, J. P.; Duran, H.; Duran, E.; Gorrichon, L.; Donnadier, D. *Chem.—Eur. J.* **2000**, *6*, 1229−1235.
(50) Barrera-Garcia, D. V.; Chassagne, D.; Paulin, C.; Raya, J.; Hirschinger, J.; Voilley, A.; Bellat, J.-P.; Gougeon, D. *Langmuir* **2011**, *27*, 1038−1043.
(51) Bailey, F. E.; Koleske, V. *Alkylene Oxides and Their Polymers*; Marcel Dekker: New York, 1991.
(52) Chatterjeh, S. K.; Sethi, K. R. *J. Macromol. Sci.−Chem. A* **1983**, *21*, 1045−1052.
(53) Burgess, C. G. V.; Everett, D. H.; Nuttall, S. *Pure Appl. Chem.* **1989**, *61*, 1845−1852.
(54) Potreck, J.; Nijmeijer, K.; Kosinski, T.; Wessling, M. *J. Membr. Sci.* **2009**, *338*, 11−16.